Colloid Polym Sci 275:979–985 (1997)

ORIGINAL CONTRIBUTION

O. Manero
J.F.A. Soltero
J.E. Puig
V.M. Gonzalez-Romero

On the application of the modeling of the relaxation spectrum to the prediction of linear viscoelastic properties of surfactant systems

Received: 17 December 1996
Accepted: 1 July 1997

Dr. O. Manero (✉)
Instituto de Investigaciones en Materiales
UNAM
A.P. 70-360
México, D.F., 04510, Mexico

J.F.A. Soltero · J.E. Puig
V.M. González-Romero
Departamento de Ingenieria Quimica
Universidad de Guadalajara
Blvd. M. Garcia Barragan #1451
Guadalajara, Jal. 44430, Mexico

Abstract In this work, the linear viscoelastic properties of cetyltrimethylammonium tosilate–water system are predicted by the modeling of the relaxation spectrum. The modeled spectrum of relaxation times is of the "wedge-box" type where the "wedge" portion is located at the short-time scale of relaxation times and the "box" part covers the long-time scale. The linear viscoelastic properties are calculated through the exact relationships with the suggested spectrum. Agreement between the calculated expressions and experimental data of the moduli and the stress relaxation function is found. Comparison is also made with predictions of the empirical expressions of the Cole–Cole and the Williams–Watts models.

Key words Relaxation spectrum – linear viscoelasticity – surfactants – dispersions – worm-like micelles

Introduction

The relaxation spectra of CTAB/NaSal solutions with varying surfactant and salt concentration were examined by Shikata et al. [1]. With increasing the salt/surfactant ratio, this system exhibits a transition from a behavior similar to that of low-molecular-weight polymer solutions in which the polymer chains are not entangled, into a behavior similar to that of high-molecular-weight polymer solutions in which the chains are fully entangled. The pronounced viscoelasticity observed at high salt/surfactant ratios suggests that threadlike micelles entangle and form networks similar to those found in flexible polymer systems [2]. These changes in the rheological behavior of the CTAB/NaSal system are accompanied by dramatic modifications in the relaxation spectra of the solutions. For instance, at surfactant concentration around 0.1 M and a salt/surfactant ratio of 0.263, the relaxation spectrum is of the "wedge" type or "Rouse–wedge" type often observed in unentangled flexible polymer chains. As the salt-surfactant concentration ratio increases, the spectrum changes into a "box" type with a plateau height G_N^0. This corresponds to the presence of entanglements in the system. At the highest ratios, the spectrum exhibits a strong peak with height G_N^0 that appears at the time scale of a single relaxation time corresponding to the Maxwell behavior. The magnitude of the relaxation time depends on the salt/surfactant ratio. At sufficiently low surfactant concentrations but with a high salt/surfactant ratio, the spectrum is composed of two regions: a Maxwell-type peak located at longer times with a relaxation time whose magnitude depends on the salt/surfactant ratio, and a ratio-independent Rouse–wedge portion at shorter times. Cole–Cole plots exhibit extra tails in the high-frequency side as well [1].

Recently, the rheological behavior of solutions of cetyltrimethylammonium tosilate (CTAT)–water [3] and its relation to phase behavior [4] were examined. The rheological behavior is dominated by a single relaxation time in the terminal zone and up to the plateau region. At higher frequencies, additional relaxation mechanisms or "breathing modes" occur, and along this region the moduli dependence on the applied frequency

Colloid & Polymer Science, Vol. 275, No. 10 (1997)

is a function of the surfactant concentration: at relatively low concentrations, a slope near one on a log–log plot of the moduli versus frequency is observed, whereas at high surfactant concentrations, the slope is approximately $\frac{1}{2}$.

Despite the similarities observed in the rheological behavior of the CTAB–salt and CTAT systems, which include response in stress relaxation and onset of shear flow experiments, there are substantial differences between them. A purely Maxwell behavior with a single relaxation time has not been found in the CTAT/water system over the frequency range where such behavior is observed in the CTAB/salt solutions. However, this does not exclude a possible Maxwell behavior with CTAT solutions containing extraneous counterions. This aspect is being investigated at present.

Cole–Cole plots in the CTAT/water system show a Maxwell behavior at low frequencies. This behavior appears to be a consequence of a kinetic process of breaking and reforming of the structural units [5]. At high frequencies, deviations are observed in samples with low and intermediate concentrations. The viscous modulus goes through a minimum and then it increases again at higher frequencies. This upturn in the viscous modulus has been interpreted as a crossover to the breathing modes or Rouse modes [5].

In accordance with the CTAT–water system, the CTAB/salt system exhibits a Maxwell behavior at low frequencies when the salt/surfactant ratio is high and the surfactant concentration is low. At high frequencies, the appearance of a "Rouse–Wedge" portion of the spectrum signals a departure from this behavior. Cole–Cole plots in the CTAB/salt system at low surfactant concentrations, exhibit tails in the high-frequency side which are very similar to those observed in the CTAT/water system. These similarities motivated the present analysis. Here, the linear viscoelastic behavior of CTAT/water system is simulated by means of a "box–wedge" spectrum of relaxation times. Predictions of the frequency-dependent rheological material functions and stress relaxation are compared with experimental data available for this system [3]. In addition, these predictions are compared with those of empirical models such as the Cole–Cole and the Williams–Watts (or stretched exponential), which are useful in predicting viscoelastic properties, although the physical interpretation of the parameters of such models is difficult. The analysis of the spectrum of relaxation times, on the other hand, is more fundamental and deserves additional attention. For this purpose, it is important to apply the exact relationships of linear viscoelastic theory to a model which represents adequately the data rather than to analyze data with approximate, empirical models.

The relaxation spectrum

Predictions of the linear viscoelastic properties for flexible polymers by modeling the relaxation spectrum have been analyzed extensively [6, 7]. In the case of entangled elongated micelles, the linear viscoelastic behavior may be described in terms of sets of relaxation processes associated with a broad class of molecular motions. In particular, the so-called "breathing modes" appearing at high frequencies in both the CTAT and CTAB/salt systems are due to relatively fast processes that occur on a length scale smaller than the dimension of the particular micellar structure.

The spectrum of relaxation times of the CTAT–water system micellar solutions may be regarded as consisting of two distinct subsets, one related to short-time processes or "breathing modes" responsible for the transition zone, and another related to long-time processes that give rise to the viscoelastic behavior in the plateau and the terminal zones. The short-time processes have a representative time τ_g which signals the high-frequency limit of the transition behavior and the onset of the so-called glassy zone in polymers. The long-time processes are represented by a longest relaxation time τ_1 which determines the transition from the terminal to the plateau zone.

The similarities of the Cole–Cole plots of the CTAB/salt/water (when the CTAB concentration is low and the salt/surfactant ratio is large) and those of the CTAT/water systems suggest that a combination of a "box-type" spectrum with a plateau height G_N^0 for long times and a "wedge-type" spectrum at short times is the correct choice for predicting the rheological functions. The viscoelastic properties are then governed by a maximum relaxation time, τ_1, a shorter relaxation time, τ_g, and a transition characteristic time, τ_2. The proposed spectra are shown in Fig. 1.

Dependences of the plateau and glassy moduli on the spectra shown in Fig. 1 are given by [2]

$$G_N^0 = \int_{\tau_2}^{\tau_1} H_1(\tau)\, d\ln\tau \,, \tag{1}$$

$$(G_g - G_N^0) = \int_{\tau_g}^{\tau_2} H_2(\tau)\, d\ln\tau \,, \tag{2}$$

where

$$H(\tau) = H_1(\tau) + H_2(\tau) \,. \tag{3}$$

The rheological functions (complex modulus and stress relaxation modulus) in terms of the spectrum for a Maxwell element are given by

$$G_1^*(\omega) = \int_{\tau_g}^{\tau_1} H(\tau) \frac{i\omega\tau}{1 + i\omega\tau}\, d\ln\tau \,, \tag{4}$$

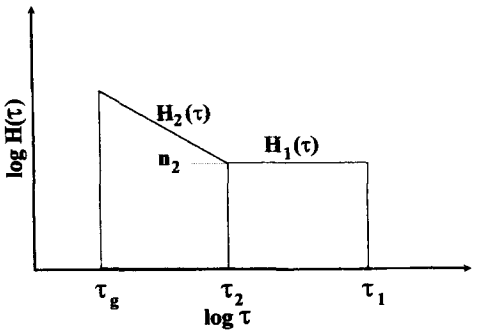

Fig. 1 Wedge–box spectra

$$G(t) = \int_{\tau_g}^{\tau_1} H(\tau) e^{(-t/\tau)} d\ln\tau \,. \tag{5}$$

At long times, the "box spectrum" is defined as

$$H_1(\tau) = \begin{cases} H_0, & \tau_2 < \tau < \tau_1 \,, \\ 0, & \tau < \tau_2,\ \tau > \tau_1 \,. \end{cases} \tag{6}$$

H_0 can be expressed in terms of τ_1, τ_2, and the viscoelastic constants through the normalization condition (Eq. (1)) [7]. This requires that

$$G_N^0 = H_0 \int_{\tau_2}^{\tau_1} d\ln\tau \,, \tag{7}$$

which gives the normalized spectrum:

$$H_1(\tau) = \frac{G_N^0}{\ln(\tau_1/\tau_2)}, \quad \tau_2 < \tau < \tau_1 \,. \tag{8}$$

Combining Eq. (8) with Eq. (4) for the box spectrum gives

$$G_1^*(\omega) = \frac{G_N^0}{\ln(\tau_1/\tau_2)} \int_{\tau_2}^{\tau_1} \frac{i\omega\tau}{1+i\omega\tau} d\ln\tau \,, \tag{9}$$

$$G_1(t) = \frac{G_N^0}{\ln(\tau_1/\tau_2)} \int_{\tau_2}^{\tau_1} e^{-t/\tau} d\ln\tau \,. \tag{10}$$

The elastic (G') and viscous (G'') moduli can be obtained from Eq. (9):

$$G_1'(\omega) = \frac{G_N^0}{2\ln(\tau_1/\tau_2)} \ln\frac{1+\omega^2\tau_1^2}{1+\omega^2\tau_2^2} \,, \tag{11}$$

$$G_1'(\omega) = \frac{G_N^0}{\ln(\tau_1/\tau_2)} [\arctan(\omega\tau_1) - \arctan(\omega\tau_2) \,. \tag{12}$$

Similarly, it is possible to obtain the power-law index of the dependence of the dynamic viscosity on frequency:

$$\frac{d\log\eta'}{d\log\omega} \approx \left[\left(\frac{\tau_1\omega}{1+\omega^2\tau_1^2} - \frac{\tau_2\omega}{1+\omega^2\tau_2^2} \right) \Big/ (\arctan(\omega\tau_1) - \arctan(\omega\tau_2)) \right] - 1 \,. \tag{13}$$

As the frequency increases, the power-law index tends to zero so the slope approaches -1. This corresponds to the existence of a limiting stress in steady-shear flow. This behavior has been observed in shear curves of liquid crystals dispersions [8].

For stress relaxation, integration of Eq. (10) yields

$$G_1(t) = \frac{G_N^0}{\ln(\tau_2/\tau_1)} \left[Ei\left(-\frac{t}{\tau_1}\right) - Ei\left(-\frac{t}{\tau_2}\right) \right], \tag{14}$$

where $Ei(x)$ is the exponential integral of x.

At short times, the "wedge-type" spectrum can be defined as

$$H_2(\tau) = \begin{cases} k_2(\tau/\tau_2)^n, & \tau_g \le \tau \le \tau_2 \ (n \text{ negative}) \,, \\ 0, & \tau < \tau_g,\ \tau > \tau_2 \,. \end{cases} \tag{15}$$

As in the box spectrum, the value of k_2 is determined by normalization. In this case, substitution of Eq. (15) into Eq. (2) gives $k_2 = n(G_g - G_N^0)/[(\tau_2/\tau_g)^n - 1]$, and the normalized spectrum $H_2(\tau)$ is given by

$$H_2(\tau) = \begin{cases} \dfrac{n(G_g - G_N^0)}{[(\tau_2/\tau_g)^n - 1]} \left(\dfrac{\tau}{\tau_g}\right)^n, & \tau_g \le \tau \le \tau_2 \ (n \text{ negative}) \,, \\ 0, & \tau < \tau_g,\ \tau > \tau_2 \,. \end{cases} \tag{16}$$

Similarly, as in the long-time subset, the complex modulus corresponding to the short-time subset is given by

$$G_2^*(\omega) = \frac{n(G_g - G_N^0)}{[(\tau_2/\tau_g)^n - 1]} \int_{\tau_g}^{\tau_2} \frac{i\omega\tau}{1+i\omega\tau} \left(\frac{\tau}{\tau_g}\right)^n d\ln\tau \,. \tag{17}$$

The contributions of this subset to the storage and loss moduli can be expressed as

$$G_2'(\omega) = \frac{n(G_g - G_N^0)}{[(\tau_2/\tau_g)^n - 1]} \left[(\omega\tau_2)^{-n} \int_0^{\omega\tau_2} \frac{u^{n+1}}{1+u^2} du - \left(\frac{\tau_2}{\tau_g}\right)^n (\omega\tau_g)^{-n} \int_0^{\omega\tau_g} \frac{u^{n+1}}{1+u^2} du \right], \tag{18}$$

$$G_2''(\omega) = \frac{n(G_g - G_N^0)}{[(\tau_2/\tau_g)^n - 1]} \left[(\omega\tau_2)^{-n} \int_0^{\omega\tau_2} \frac{u^{n}}{1+u^2} du - \left(\frac{\tau_2}{\tau_g}\right)^n (\omega\tau_g)^{-n} \int_0^{\omega\tau_g} \frac{u^{n}}{1+u^2} du \right]. \tag{19}$$

At high frequencies, the hypergeometric integrals have the following limits:

$$\int_0^{\infty} \frac{u^{n+1}}{1+u^2} du = \frac{\pi}{2} \operatorname{cosec}\left(\frac{n\pi}{2}\right), \quad -1 < n < 0 \,, \tag{20}$$

$$\int_0^{\infty} \frac{u^{n}}{1+u^2} du = \frac{\pi}{2} \sec\left(\frac{n\pi}{2}\right), \quad -1 < n < 0 \,. \tag{21}$$

Colloid & Polymer Science, Vol. 275, No. 10 (1997)

The elastic and viscous moduli of the full spectrum are the sum of the contributions from the short and long relaxation times:

$$G'(\omega) = G'_1(\omega) + G'_2(\omega)\,, \tag{22}$$

$$G''(\omega) = G''_1(\omega) + G''_2(\omega)\,. \tag{23}$$

The contribution of the wedge spectrum to the stress relaxation is small and corresponds to a time scale much lower than that of the experiments. For this case

$$G(t) \approx G_1(t)\,. \tag{24}$$

The empirical Cole–Cole equation has been used to predict the moduli behavior along the transition region. This reads

$$G^*_{DC}(\omega) = G^0_N + \frac{G_g - G^0_N}{1 + (i\omega\tau)^\beta}\,, \tag{25}$$

where τ is a characteristic time and β the empirical parameter ($0 < \beta \leq 1$). The elastic and viscous moduli corresponding to Eq. (25) are

$$G'_{DC}(\omega) = G^0_N + (G_g - G^0_N)\frac{1 + (\omega\tau)^\beta \cos(\beta\pi/2)}{1 + 2(\omega\tau)^\beta \cos(\beta\pi/2) + (\omega\tau)^{2\beta}}\,, \tag{26}$$

$$G''_{DC}(\omega) = (G_g - G^0_N)\frac{(\omega\tau)^\beta \operatorname{sen}(\beta\pi/2)}{1 + 2(\omega\tau)^\beta \cos(\beta\pi/2) + (\omega\tau)^{2\beta}}\,. \tag{27}$$

Along the transition zone the moduli behave as

$$G'_{DC} \approx G^0_N + (G_g - G^0_N)(\omega\tau)^\beta \cos\left(\frac{\beta\pi}{2}\right), \tag{28}$$

$$G''_{DC} \approx (G_g - G^0_N)(\omega\tau)^\beta \sin\left(\frac{\beta\pi}{2}\right). \tag{29}$$

It is noteworthy that Eqs. (28) and (29) behave like Eqs. (18) and (19) in the high-frequency limit, provided that $\tau_2/\tau_g \to \infty$

$$G'_2(\omega) \approx \left(\frac{n\pi}{2}\right)(G_g - G^0_N)(\omega\tau_g)^{-n} \operatorname{cosec}\left(\frac{n\pi}{2}\right), \tag{30}$$

$$G''_2(\omega) \approx \left(\frac{n\pi}{2}\right)(G_g - G^0_N)(\omega\tau_g)^{-n} \sec\left(\frac{n\pi}{2}\right). \tag{31}$$

In fact, the slope of the transition zone is the same for both sets of Eqs. (28), (29), (30) and (31)

$$\lim_{\omega\to\infty} \frac{G''_2(\omega)}{G'_2(\omega)} = \frac{\sec(n\pi/2)}{\operatorname{cosec}(n\pi/2)} = \tan(n\pi/2), \quad -1 < n < 0 \tag{32}$$

$$\lim_{\omega\to 0} \frac{G''_{DC}(\omega)}{G'_{DC}(\omega)} = \tan(\beta\pi/2)\,, \tag{33}$$

which shows that the parameter β is equal to the slope ($-n$) of the wedge spectrum in Fig. 1.

In a similar fashion, the predictions of the empirical expression used to fit data of stress relaxation experiments (the so-called Williams–Watts equation) can be compared with Eq. (14). The W–W equation is

$$G_{ww}(t) = G^0_N \exp(-t/\tau_0)^\alpha\,. \tag{34}$$

Results

The model is validated by comparing its predictions with experimental data of the CTAT–water system and with predictions of the above-mentioned empirical models. The CTAT–water system was examined in a wide concentration range. As discussed elsewhere [3], experimental results show an upturn in G'' at frequencies higher than 50 rad/s, which has been interpreted in terms of a crossover between the regimes of reversible scission (Maxwell behavior) and that of breathing of the polymer-like micelles. Within this frequency range, G'' shows a larger frequency dependence as the concentration decreases [3]. Experiments suggest that the slope of log moduli versus log frequency in the transition zone at low concentrations is close to one and that at higher concentrations is approximately $\frac{1}{2}$. Since the slope in the transition region corresponds to the negative of n in the wedge spectrum, values of 0.5 and 0.95 were given to the slopes in the high-concentration and low-concentration ranges, respectively. As shown elsewhere [3], the dependence of the dynamic viscosity with frequency in the moderate frequency range reaches a limiting slope of -1 in a log–log plot. This corresponds to an almost constant G'' in the plateau region, which is characteristic of a box spectrum at long times. However, for frequencies in the transition region, the slope of $\log G''$ versus $\log\omega$ is close to 1, which corresponds to a second Newtonian plateau of η' at high frequencies usually observed in dispersions. This is observed in the experimental results shown in [3] for the low and moderate concentration samples, i.e., for samples with CTAT concentrations smaller than 15%.

Predictions of the moduli for the box–wedge spectra require the values of G_g, G^0_N, n and the characteristic times τ_1, τ_2 and τ_g. All of them except G_g and τ_g, may be evaluated from the experimental data. The product $G_g\tau_g$ is the high-frequency viscosity limit (η_∞), which has been described in theoretical analyses of flowing dispersions of

Table 1 Parameters used in the modeled spectra

wt% CTAT	τ_1 [s]	τ_2 [s]	$\tau_g \times 10^8$ [s]	G^0_N [Pa]
10	1.335	0.511	3.589	216.7
20	0.43	0.175	0.221	718.3

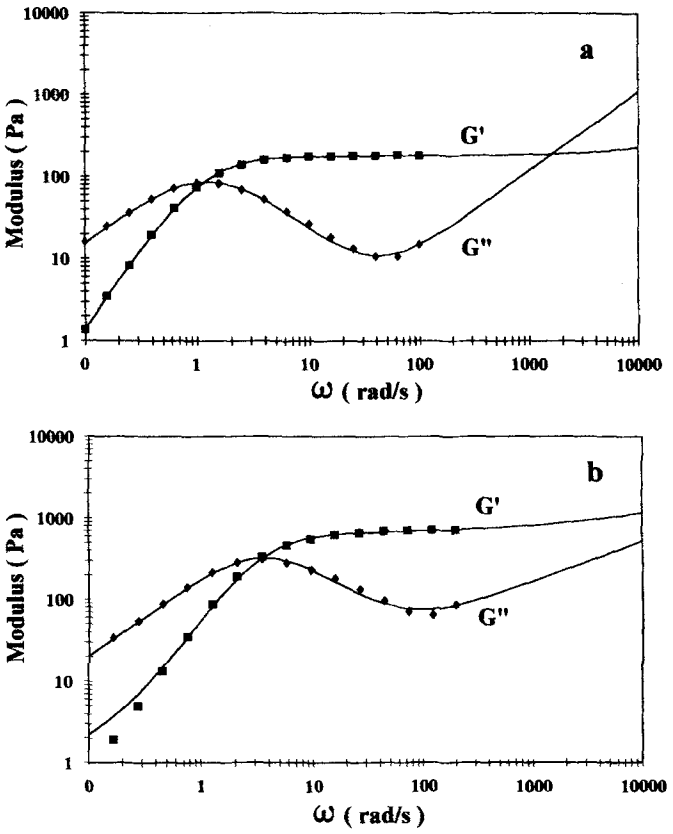

Fig. 2 Experimental data and theoretical predictions for the CTAT–water systems at two concentrations; (a) 10 wt%; (b) 20 wt%

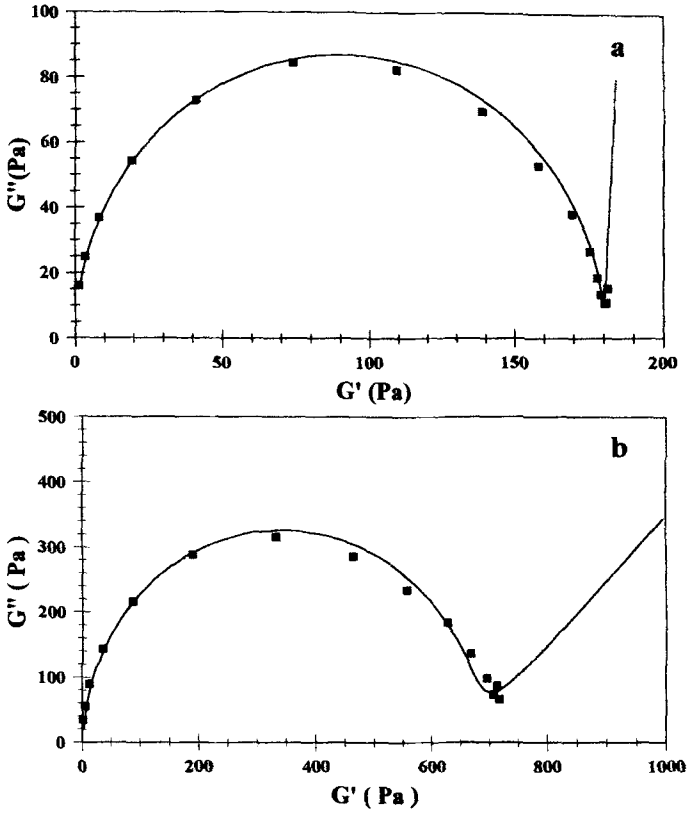

Fig. 3 Cole–Cole plots depicting experimental data and theoretical predictions for the same systems shown in Fig. 2

particulate systems in the high-frequency range of the spectrum [9]. In dilute to moderate dispersions, η_∞ may have a magnitude close to that of the solvent viscosity. Since Eqs. (18) and (19) require independent values of G_g and τ_g, those were estimated by setting $\eta_\infty \approx 0.001$ Pa s and $G_g \approx 100 G_N^0$. Table 1 shows the model parameters used to predict the variations of the moduli with frequency.

Predictions of the box–wedge spectra for the moduli are given in Fig. 2, together with the experimental data. In the transition region, the Cole–Cole equation and the predictions of the wedge spectrum coincide. This figure shows a good agreement with experiments for surfactant concentrations of 10% and 20%, respectively. For concentrations larger than about 25 wt% surfactant, a transition into a single liquid-crystalline-phase occurs. Disagreement with experiments indicates that the rheological functions, especially G'', do not follow a box-type spectrum but a more general wedge-type in the plateau and transition regions.

Cole–Cole diagrams corresponding to data depicted in Fig. 2 are shown in Fig. 3. At low concentrations (Fig. 3(a)), predictions agree well with experiments at the beginning of the transition region. For the higher concentrations (Fig. 3(b)), predictions of the semicircle are also in good agreement with experiments.

The stretched-exponential and box spectrum predictions are compared with experimental data over an extended time scale in Fig. 4. Comparison with a single-exponential relaxation behavior is also made. Along the experimental time-range, data can be fitted by a single exponential, as shown also elsewhere [3]. However, over an extended time range, the prediction of the box spectrum deviates from those of a single exponential. Eqs. (14) and (34) coincide well when $\tau_0 = \tau_1$, although the value assigned to α is arbitrary. In Fig. 4(a) (low-concentration sample) predictions of the box spectrum and of the stretched exponential are very near to those of a single-exponential relaxation. When the surfactant concentration is increased, deviations from the single-exponential behavior are apparent at long times, but both the stretched exponential and the box-spectrum curves coincide. Values of the empirical parameter α in the stretched exponential varied between 0.75 in the 10% sample and 0.9 for the 20% sample, respectively.

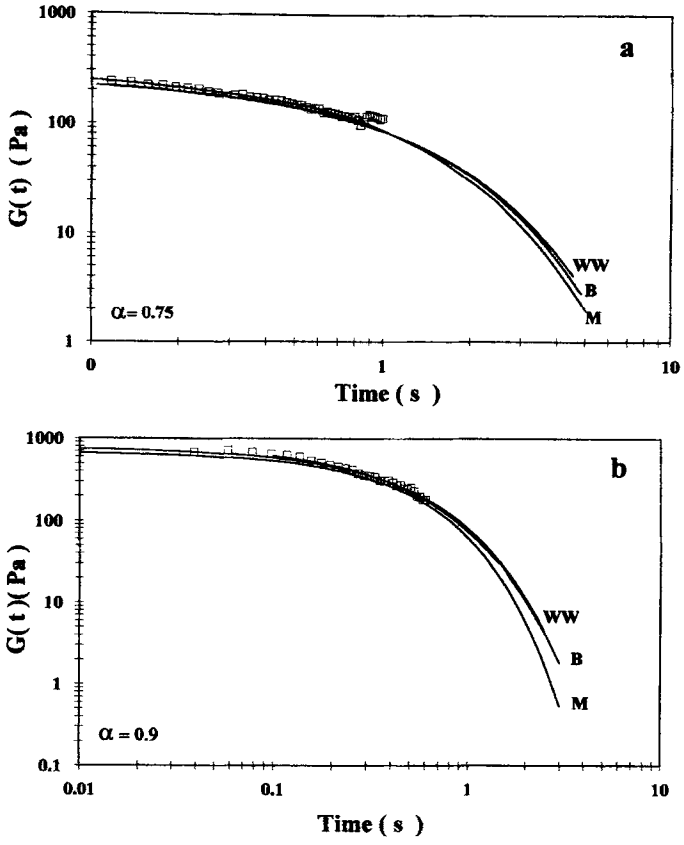

Fig. 4 Experimental data and theoretical predictions of the variation of the relaxation modulus with time for the same systems depicted in Fig. 2. Predictions of the Williams–Watts (WW), Maxwell (M) and box spectrum (B) are shown

Discussion and conclusions

The linear viscoelastic behavior of the CTAT–water systems was analyzed at various surfactant concentrations ranging from dilute ($c \leq 10\%$) to concentrated solutions ($c = 20\%$) close to the transition into a hexagonal phase [3]. Changes in the rheological behavior of such solutions are substantial, especially in the transition region of the spectra where the slopes of the moduli vs. frequency in a log–log plot vary from almost one to $\frac{1}{2}$ as the CTAT concentration is increased. Systems at relatively low concentration were modeled by the Hess model for surfactants [9], which predicts a slope of one at the beginning of the transition zone. With increasing concentration, within this region, the slope changes into a Rouse-like behavior with a smaller slope. It is clear that increasing steepness of the slope of the wedge-type spectrum at short times in the transition zone will be accompanied by a compression of the transition from rubber-like to glass-like consistency into a narrower region in logarithmic frequency scale. In this case τ_g is smaller in the more dilute systems. Moreover, the behavior of the viscoelastic functions in the low-frequency end of the transition zone will depend not only on the shape of the spectrum but also on the density of the entanglement network. Increasing G_N^0 compresses the magnitudes of the moduli in the transition region. In this regard, a trend towards a steeper slope is observed in the transition zone of the spectrum with increased dilution in flexible polymers [2]. This behavior is similar to that observed in the CTAT systems analyzed here.

Besides data presented here for CTAT systems, Thurn et al. [8] analyzed the rheological behavior of tetradecyl pyridinium salicylate and tetradecyltrimethylammonium salicylate. Results show a slope close to one for G'' at the beginning of the transition zone. Data were simulated by the Hess model [9] with an expression for the viscous modulus in the high-frequency zone of the plateau-transition region of the following form:

$$G''(\omega) = G_N^0 \frac{\omega\tau_\varepsilon}{1 + (\omega\tau_\varepsilon)^2} + \eta_\infty\omega \,, \tag{35}$$

where τ_ε is the largest relaxation time and η_∞ the high-shear limit of the viscosity. The first term in Eq. (35) corresponds to Maxwell-like spectrum. The second term may be identified with the expression (31) by making η_∞ proportional to $(G_g - G_N^0)\tau_g$. It predicts the behavior of G' and G'' quite well over the whole range of frequencies for samples of low concentrations. In this model, there is an additional term to the Maxwell expression for the loss modulus which corresponds to the influence of the alignment tensor of the constitutive units. This quantity $(\eta_\infty\omega)$ is proportional to the energy associated with the alignment of the particles or units influenced by the neighboring particles, where η_∞ represent the viscosity at high frequencies which was chosen here as a fitting parameter in the predictions of the experimental data. The consequence of the presence of this term is the linear variation of G'' with ω at high enough frequencies which follows closely the observed upturn in the experiments at higher frequencies. This effect leads to a stronger frequency dependence than in the Rouse regime. In this form, this identification provides a molecular explanation to some parameters of the wedge spectrum at low concentrations. At higher concentrations, for example 30 wt% CTAT, the change in the long-time spectrum from a box type into a more general wedge type has also been observed in the CTAB/NaSal system studied by Shikata et al., when the surfactant concentration is high and the salt/surfactant ratio is relatively low.

Finally, results of the simulation of the viscoelastic spectra for surfactant systems presented in this paper have illustrated the relationships between the parameters of molecular models (such as the Hess model) and those of the spectra of relaxation times. In addition, a comparison of the modeled spectra with empirical models may provide a physical basis for the parameters of these models.

References

1. Shikata T, Hirata H (1987) Langmuir 3:1081
2. Ferry JD (1980) Viscoelastic Properties of Polymers 3rd ed Wiley, New York
3. Soltero JFA, Puig JE, Manero O (1996) Langmuir 12:2654
4. Soltero JFA, Puig JE, Manero O, Schulz PC (1995) Langmuir 11:3337
5. Cates ME, Candeau SJ (1990) J Phys Condens Matter 2:6869
6. Frederick JE, Yeh ST, McIntyre D Weidknecht (1994) J Rheol 38:937
7. Tschoegl NW (1989) The Phenomenological Theory of Linear Viscoelastic Behavior, Springer, New York
8. Thurn H, Löbl M, Hoffmann H (1985) J Phys Chem 89:517
9. Hess SZ (1980) Naturforsch A 35A:915